Published in final edited form as:
Development. 2005 March ; 132(6): 1463–1473. doi:10.1242/dev.01658.

Ovol1 regulates meiotic pachytene progression during spermatogenesis by repressing Id2 expression

Baoan Li[1], **Mahalakshmi Nair**[1,2], **Douglas R. Mackay**[1], **Virginia Bilanchone**[1], **Ming Hu**[1], **Magid Fallahi**[1], **Hanqiu Song**[1], **Qian Dai**[1], **Paula E. Cohen**[3], and **Xing Dai**[1,2,*]

[1]Department of Biological Chemistry, University of California, Irvine, CA 92697, USA

[2]Developmental Biology Center, University of California, Irvine, CA 92697, USA

[3]Department of Biomedical Science, Cornell University, Ithaca, NY 14852, USA

Summary

Previous studies have shown that a targeted deletion of *Ovol1* (previously known as *movo1*), encoding a member of the Ovo family of zinc-finger transcription factors, leads to germ cell degeneration and defective sperm production in adult mice. To explore the cellular and molecular mechanism of *Ovol1* function, we have examined the mutant testis phenotype during the first wave of spermatogenesis in juvenile mice. Consistent with the detection of *Ovol1* transcripts in pachytene spermatocytes of the meiotic prophase, *Ovol1*-deficient germ cells were defective in progressing through the pachytene stage. The pachytene arrest was accompanied by an inefficient exit from proliferation, increased apoptosis and an abnormal nuclear localization of the G2-M cell cycle regulator cyclin B1, but was not associated with apparent chromosomal or recombination defects. Transcriptional profiling and northern blot analysis revealed reduced expression of pachytene markers in the mutant, providing molecular evidence that pachytene differentiation was defective. In addition, the expression of Id2 (inhibitor of differentiation 2), a known regulator of spermatogenesis, was upregulated in *Ovol1*-deficient pachytene spermatocytes and repressed by Ovol1 in reporter assays. Taken together, our studies demonstrate a role for *Ovol1* in regulating pachytene progression of male germ cells, and identify Id2 as a *Ovol1* target.

Keywords

Ovol1 (*movo1*); Id2 (Idb2); Spermatogenesis; Germ cell differentiation; Meiosis; Pachytene; Meiotic prophase; *Drosophila ovo/svb*

Introduction

As male germ cells embark on the process of spermatogenesis, they must modify their program of gene expression to produce changes in chromatin structure, organelle content and cell shape, and coordinate these changes with the control of mitotic and meiotic divisions. The spermatogenic gene expression program uses both transcriptional and translational control mechanisms (Eddy, 2002; Sassone-Corsi, 1997). Despite abundant reports in the literature showing the expression of various transcription factors in male germ cells, functional significance in spermatogenesis has only been established for a subset of them (Eddy, 2002).

*Author for correspondence (xdai@uci.edu).

Supplementary material
Supplementary material for this article is available at http://dev.biologists.org/cgi/content/full/132/6/1463/DC1

Examples include A-myb (Mybl1 – Mouse Genome Informatics) and Egr4, which are required for male germ cell development at the meiotic prophase (Toscani et al., 1997; Tourtellotte et al., 1999); and Sprm1, Crem, Jund1 and the TBP-like factor Tlf/Trf2, which are required for postmeiotic germ cell differentiation (Blendy et al., 1996; Martianov et al., 2001; Nantel et al., 1996; Pearse et al., 1997; Thepot et al., 2000; Zhang et al., 2001).

Meiotic prophase, an extended G2 phase where germ cells transit from the mitotic to the meiotic cell cycle, is tightly regulated, particularly at pachytene, the longest stage in prophase. During prophase, chromosomes undergo dynamic behavioral changes such as movement, pairing, synapsis and recombination, and checkpoint mechanisms exist to monitor such chromosomal behavior (Cobb and Handel, 1998; Cohen and Pollard, 2001). The pachytene stage is also when mRNA synthesis is particularly active, producing transcripts that encode proteins required for meiotic and postmeiotic germ cells (Eddy and O'Brien, 1998). Although examples of transcriptional control of meiotic pachytene progression have been documented in yeast (Chu and Herskowitz, 1998; Tung et al., 2000) and *Drosophila* (Lin et al., 1996; White-Cooper et al., 1998), studies probing such control mechanisms in mammalian gametogenesis are only beginning to appear (Eddy, 2002).

The conserved *ovo* gene family encodes DNA-binding transcription factors that lie downstream of the canonical *Wg/Wnt* signaling pathway (Li et al., 2002b; Payre et al., 1999) and control the differentiation of a number of tissues in multicellular organisms, including *C. elegans*, *Drosophila* and mice (Dai et al., 1998; Johnson et al., 2001; Oliver et al., 1990; Payre et al., 1999). Therefore, analysis of the regulation and function of *Ovo* genes provides an excellent tool with which to investigate the control mechanisms required for cellular differentiation processes in a complex tissue setting, and to examine how these mechanisms evolve (Sucena et al., 2003; Wang and Chamberlin, 2002).

Three distinct mouse *ovo* family genes, *Ovol1*, *Ovol2* (previously known as *movo2* or zinc finger protein 339) and *Ovol3* (previously known as *movo3*) exist (Li et al., 2002a). Ablation of *Ovol1* in mice leads to defects in several tissues that express *Ovol1*, including testis, skin, kidney and the urogenital tract (Dai et al., 1998). Female mutant mice showed reduced fertility primarily due to structural defects in the urogenital tract; however, no apparent abnormalities were observed in oogenesis. Defects are most severe and of highest penetrance in the testis, where a dramatic decrease in production of spermatozoa, in testis weight and in male fertility was observed. Although this study suggested a role for *Ovol1* in sperm production, the primary function and cellular target(s) of *Ovol1* in spermatogenesis was not defined due to complications from secondary events such as massive germ cell degeneration in the adult mutant testis. In the present study, we examined the first, relatively synchronous, round of spermatogenesis that spans the first several postnatal weeks to reveal the primary consequences of the absence of a functional *Ovol1* gene. We report that *Ovol1* is expressed during the pachytene stage of meiotic prophase and is a crucial regulator of pachytene progression of male germ cells. We also provide molecular evidence suggesting that Id2 is a *Ovol1* target.

Materials and methods

Northern blot analysis

Total RNA was isolated from paired testes and northern blot analysis was performed as described (Dai et al., 1998). The following cDNA probes were used: a 350 bp fragment containing the 5′ UTR of *Ovol1*; a 320 bp PCR fragment containing sequences in exons 2 and 3 of *Ovol2*; a 608 bp fragment corresponding to nucleotides 1791-2399 of Adam2 mRNA (Accession Number MMU22057); a 417 bp fragment corresponding to nucleotides 297-714 of Tctex-2 mRNA (Accession Number M26332); a 400 bp fragment corresponding to nucleotides 763-1163 of S-II-T1 cDNA (Accession Number NM-009326); a 429 bp fragment

corresponding to nucleotides 1896-2325 of Odf2 mRNA (Accession Number NM-013625); a 590 bp fragment corresponding to nucleotides 64-654 of cyclin B1 mRNA (Accession Number S43105); a 457 bp fragment corresponding to nucleotides 4-460 of Cdc2 mRNA (Accession Number BC024396); and a 406 bp fragment containing sequences corresponding to 1062-1468 of Id2 mRNA (Accession Number AF077860).

In situ hybridization

Digoxigenin-labeled sense and antisense cRNA probes were synthesized from either an 870 bp *Ovol1* fragment containing the 3′ UTR region, a 1.6 kb *Ovol2* cDNA fragment representing a nearly full-length transcript, or a 754 bp fragment corresponding to nucleotides 11-764 of Id2 mRNA (Accession Number NM_010496). The in situ hybridization procedure was adapted from Deng and Lin (Deng and Lin, 2002). Specifically, freshly dissected testis samples were fixed in 4% paraformaldehyde/PBS overnight at 4°C and subsequently passed through a series of sucrose/PBS solutions of increasing sucrose concentration (10%, 15%, 20% and 30%). After an overnight incubation in 30% sucrose/PBS:OCT (1:1), the samples were frozen in 30% sucrose/PBS:OCT (1:3). Sections (8 μm) were cut and dried at 50°C for 2 hours, followed by drying at room temperature overnight. Dried sections were stored at −80°C until use in subsequent in situ hybridization experiments. Thawed sections were treated with proteinase K (30 μg/ml in PBS) for 5 minutes at room temperature, rinsed briefly in PBS, and re-fixed in 4% paraformaldehyde/PBS for seven minutes. Following post-fixation washes, the appropriate digoxigenin-labeled probes were added to the slides at a concentration of 1 μg/ml in hybridization buffer (1.3×SSC, 50% formamide, 5 mM EDTA, 0.5% CHAPS, 100 μg/ml heparin, 50 μg/ml yeast RNA, 0.5% Tween-20, pH 6.5) and allowed to hybridize at 60°C overnight. The slides were then washed in several changes of 0.2×SSC, 50% formamide at 60°C over a period of 1 hour. Immunological detection of digoxigenin-labeled probes was performed by incubating the slides with a α-digoxigenin-AP conjugated antibody [diluted 1:2000 in a buffer containing 2% blocking reagent (Roche), 2% normal goat serum, 100 mM Tris-Cl, 150 mM NaCl, 0.5 mg/ml levamisole, pH 7.5] for 3 hours at room temperature, followed by a colorimetric reaction using the NBT/BCIP substrates. Counterstaining with the α-Ldhc4 antibody was performed using a 1:100 dilution in 10% normal goat serum/PBS at room temperature for 1 hour followed by incubation in a 1:100 dilution of a α-rabbit-FITC conjugated antibody at room temperature for 1 hour.

BrdU labeling

Juvenile male mice were injected intraperitoneally with BrdU (5-Bromo-2′-deoxyuridine, Sigma B5002) at a dose of 50 μg/g body weight, sacrificed 2 hours after injection, and their testes dissected and fixed in Bouin's fixative as described above. Paraffin sections were incubated in a 60°C oven overnight, and deparaffinized by a 5-minute wash with Histoclear and rehydrated by a series of rinses in decreasing concentrations of ethanol (100%, 95%, 70%, 50%, 0%). The slides were then treated with 50% formamide in 2×SSC at 65°C for 2 hours, followed by two 5-minute rinses in 2×SSC, and incubation in 2N HCl at 37°C for 30 minutes. Samples were neutralized by incubating in 0.1 M boric acid, pH 8.5 for 10 minutes, rinsed briefly in PBS and endogenous peroxidase was quenched by incubating in freshly prepared 3% H_2O_2 for 15 minutes. After three 5-minute washes in PBS, samples were subjected to immunohistochemical analysis as described above using a mouse monoclonal α-BrdU antibody (Roche). The BrdU-positive cells in P14 mutant and wild-type testes were counted, and the total number in an area of 2×10^5 μm^2 in size (equivalent to ~30 tubular cross-sections) was calculated as an average of three independent areas.

Histology, immunofluorescence and immunohistochemistry

Testis samples of the desired ages (P14-P21) were fixed in Bouin's fixative for 12-24 hours, depending on tissue size, processed and embedded in paraffin wax. Sections (5 μm) were stained with the periodic acid/Schiff sulfite leucofuchsin (PAS) reaction, Hematoxylin and Eosin, or the appropriate antibodies. Immunofluorescence using a polyclonal rabbit α-Ldhc4 antibody (Hintz and Goldberg, 1977), a guinea pig α-histone H1t (Inselman et al., 2003), or a monoclonal mouse α-cyclin B1 antibody (Santa Cruz Biotechnology), was as described (Dai et al., 1998). Immunohistochemistry using a rat IgM α-mouse Gcna1 monoclonal antibody (Enders and May, 1994) was performed using the SABC kit (Zymed) or the VECTASTAIN elite ABC kit (Vector) according to the manufacturer's recommendations.

Detection of apoptosis

The terminal deoxynucleotidyl transferase-mediated dUTPdigoxigenin nick end-labeling (TUNEL) assay was used to detect apoptotic germ cells. Frozen testis sections from 21-day-old mice were fixed in 4% paraformaldehyde for 10 minutes at room temperature, followed by three 5-minute washes in PBS. Sections were then processed using the In Situ Cell Death Detection Kit according to the manufacturer's recommendations (Roche)

Chromosome analysis

Preparation of spermatocyte spreads and the analysis of prophase I chromosomes by immunostaining of chromosome-associated proteins were as described (Edelmann et al., 1999; Kneitz et al., 2000).

Transcriptional profiling

Three identical experiments were performed independently. In each experiment, testes from two to four *Ovol1*$^{-/-}$ mice together with two to four wild-type control littermates were taken for RNA preparation, and total RNA pooled from testes of the same genotype. Total RNA (2 μg) from each sample group was reverse-transcribed into cDNA, which was then transcribed into biotin-labeled cRNA (Zhao et al., 2000). Labeled cRNA (15 μg) was used in each hybridization to Affymetrix Murine 11K Genechips (SubA and SubB) covering ~11,000 genes and ESTs. The Affymetrix GeneChip Analysis Suite software (MAS 4.0) was used to generate the raw data report. For each entry on the microarray, the software calculates an average of the difference between perfect-match and mismatch probes (up to 20 probes per gene). This so-called average difference is directly related to the level of expression of the transcript, and is normalized between chips by the use of a global target value for total chip fluorescence. The program also carries out a combinatorial evaluation of the performance of each probe set using several analysis metrics to determine the presence or absence of each transcript. Raw data were further analyzed using the CyberT program (Long et al., 2001), which runs a T test on the three data sets of the Affymetric output in Excel format and includes features to allow Bayesian-based approximations of standard deviations for measurements.

Reporter assays

293T cells were seeded in 24-well plates and transfected at 12-15% confluence with Ca^{2+} phosphate as described (Pear et al., 1993). A typical transfection mixture contained a total of 0.5 μg of plasmids, including: 50 ng of pGL3-Id2 (where a 1148-bp Id2 gene regulatory fragment was cloned upstream of the luciferase reporter gene); 0, 5, 10, 15 or 20 ng of the *Ovol1* expression vector (pCB6-Ovol1) (Dai et al., 1998); and 0.04 mg of a β-actin promoter-β-gal construct. Or a total of 0.5 μg of plasmids, including: 10 ng of pGL3-Id2; and 0, 10, 20, 40 or 70 ng of the VP16-Ovol1-expressing vector; and 0.04 μg of a β-actin promoter-β-gal construct. pCB6 (+) (empty vector containing the CMV promoter) was used as stuffer DNA. Luciferase activity was measured in whole cell extracts using the Luciferase Assay System

(Promega). β-Galactosidase activity was measured as previously described (Eustice et al., 1991).

Results

Pachytene-specific activation of *Ovol1* expression in adult and prepubertal testis

To precisely define the onset of *Ovol1* expression during spermatogenesis, we performed in situ hybridization experiments using an *Ovol1* probe, with the same sections immunostained with an antibody to Ldhc4, a germ cell marker that is normally expressed from mid/late-pachytene stage onwards (Hintz and Goldberg, 1977). In adult testis, the level of *Ovol1* transcripts varied from one seminiferous tubule to another (Fig. 1A,C), indicating that *Ovol1* expression is seminiferous tubule cycle-dependent. The onset of *Ovol1* expression coincided with that of Ldhc4 protein synthesis (Fig. 1B,D), suggesting a mid/late-pachytene-specific activation of *Ovol1* transcription. *Ovol1* transcripts were present from mid/late-pachytene spermatocytes to round spermatids, but were not detected in elongate spermatids or in germ cells prior to the pachytene stage.

We next examined *Ovol1* expression during prepubertal testis development, which spans the first four or five postnatal weeks. Postnatal day 16 (P16, with the day of birth considered P0) is when the most advanced germ cells have reached the mid/late-pachytene stage; in situ hybridization of P16 testis revealed the presence of *Ovol1* transcripts in the Ldhc4-expressing pachytene spermatocytes (Fig. 1E,F). Furthermore, levels of *Ovol1* mRNA increased between P14 and P21, consistent with the appearance of mid/late-pachytene spermatocytes within this developmental window (Bellve et al., 1977) (Fig. 1G). Therefore, *Ovol1* expression is activated in pachytene spermatocytes during the first round of spermatogenesis and in adult testis.

Inefficient exit from proliferation, incomplete pachytene arrest, and increased apoptosis in *Ovol1*$^{-/-}$ testis

Meiotic pachytene is a key stage in yeast meiosis after which point a decision to exit mitosis becomes irreversible (Shuster and Byers, 1989). The expression of *Ovol1* in pachytene spermatocytes led us to examine whether exit from proliferation might be affected in prepubertal *Ovol1*$^{-/-}$ testis. A small number of mutant tubules contained multiple layers of bromodeoxyuridine (BrdU)-labeled germ cells (arrows in Fig. 2B), whereas in wild-type mice at this age such proliferating cells only occupy the outermost layer (spermatogonia) of the tubule. This said, there was only a very slight increase (~7%) in the actual number of BrdU-positive cells in the mutant testis (not shown). These results suggest that *Ovol1* is not essential for germ cell proliferation per se, but probably plays a modulatory role in the ability of a germ cell to exit mitosis.

To determine if *Ovol1* is required at the meiotic prophase and/or subsequent stages, we compared the morphology of *Ovol1*$^{-/-}$ and control testis between the ages of two and three postnatal weeks. At P14, when the most advanced stage is early/midpachytene, comparable levels of pachytene spermatocytes, representing about 13-14% of the total germ cells, were present in the lumen of both control and *Ovol1*$^{-/-}$ seminiferous tubules (Fig. 2C,D; Table 1). At P16 in wild-type mice, spermatocytes had reached the late-pachytene stage (as judged by the large size of their nuclei or the presence of ‘sex bodies’ containing the XY chromosomes) (Fig. 2E). By contrast, mutant tubules at this time contained only about one half the number of spermatocytes that showed a late-pachytene appearance (Fig. 2F; Table 1). Interestingly, the total number of pachytene spermatocytes (sum of early/mid- and late-pachytene) was not significantly affected (Table 1), indicating a compensatory increase in the number of early/mid-pachytene spermatocytes (see below). Thus, in the absence of a functional *Ovol1* gene,

the first round of spermatogenesis is partially blocked during the pachytene stage of meiotic prophase.

Another characteristic feature of the mutant juvenile testis was the increased number of apoptotic cells, containing darkly stained nuclei lacking discernible chromosome structure (Dix et al., 1997). Such cells began to appear at P16 (Fig. 2F), but were frequently observed at P21 (Fig. 2H-J). TUNEL assays confirmed that juvenile mutant testis contained significantly more apoptotic cells than the wild-type control (Fig. 2L, compare with 2K). In most cases, apoptotic cells were confined to the innermost layers of mutant tubules, at positions where normally only late-pachytene spermatocytes and more advanced germ cells such as round spermatids are found. However, not all cells that were at or after late-pachytene were eliminated by apoptosis, as more advanced germ cells with apparently normal morphology were present in the mutant, albeit reduced in number (Fig. 2J).

The pachytene arrest of *Ovol1*$^{-/-}$ germ cells was associated with aberrant marker expression but not with chromosomal or recombination defects

To further explore the pachytene defect in *Ovol1*$^{-/-}$ testis, we examined the biochemistry of prepubertal mutant and wild-type testis using antibodies to known differentiation markers. These include Gcna1, which marks the germ cells prior to midpachytene (Enders and May, 1994), and Ldhc4 and histone H1t (Cobb et al., 1999), which mark the mid/late-pachytene spermatocytes. At P14, nearly all wild-type tubules had multiple rows of Gcna1^{+} cells (Fig. 3A), whereas only very few contained Ldhc4^{+} cells (Fig. 3E). By P16, Gcna1^{+} cells were restricted to only one or two rows at the periphery (Fig. 3C), and the number of Ldhc4^{+} cells rose significantly (Fig. 3G). This switch in marker gene expression was defective in the *Ovol1*$^{-/-}$ testis, which at P16 contained more Gcna1^{+} cells and fewer Ldhc4^{+} cells than the controls (Fig. 3D,H; Table 1). Multiple rows of germ cells in the P16 *Ovol1*$^{-/-}$ tubules retained their Gcna1 expression even when they reached the lumen, and the number of Ldhc4^{+} cells was more than twofold lower than that in the control littermates. This was also true at P21 for tubules that had not yet started massive apoptosis (data not shown). Histone H1t expression overlapped that of Ldhc4 in both the mutant and control testis (Fig. 3I-L), confirming a reduction in the number of mid/late-pachytene spermatocytes in the mutant. Collectively, these results indicate that *Ovol1*-deficient germ cells are unable to efficiently progress beyond mid-pachytene, and support our morphological observation of a meiotic pachytene defect.

Cyclin B1, a key component of the M-phase-promoting factor (MPF) implicated in the regulation of meiotic G2-M transition, is normally upregulated in pachytene spermatocytes (Chapman and Wolgemuth, 1994; Cobb et al., 1999; Godet et al., 2000; Liu et al., 2000). We therefore wondered whether its expression might be affected in the *Ovol1* mutant germ cells. As shown in Fig. 4A,C, cyclin B1 protein was detected in wild-type testis in the adluminal cells that are mid-pachytene and beyond, as indicated by Ldhc4 staining. Coinciding with the progression from pachytene (at P16) to meiosis (at P21) (Bellve et al., 1977), cyclin B1 protein switched its subcellular localization from the cytoplasm (arrow in Fig. 4A) to the nucleus (arrowhead in Fig. 4C). This developmental cytoplasmic-to-nuclear switch recapitulates the observation in adult testis (Liu et al., 2000), and is consistent with the reported nuclear translocation of cyclin B1 during G2-M transition in mitotic cells (Pines and Hunter, 1991). Two abnormalities were identified in the *Ovol1*$^{-/-}$ mutant testis using double immunostaining with the cyclin B1 and Ldhc4 antibodies. First, many adluminal, *Ovol1*-deficient germ cells did not show any Ldhc4 staining but stained positive for cyclin B1 (arrowheads in Fig. 4B,H). This result suggests a developmental uncoupling of cell cycle-specific and differentiation-specific gene expression in the mutant. Second, in these Ldhc4-negative mutant spermatocytes, cyclin B1 protein was in the nucleus. This precocious nuclear localization is suggestive of either ectopic mitosis or premature meiosis.

To formally exclude the possibility that *Ovol1* is involved in premeiotic chromosomal metabolism, we examined the mutant testis for any possible chromosomal or recombination defects. The formation of synaptonemal complexes in the mutant was indistinguishable from that in wild type (data not shown), as indicated by the proper accumulation of the synaptonemal complex protein SCP3 (also known as Cor1 or Sycp3) and the central element protein SCP1 (also known as Syn1 or Sycp1) (Fig. 5A). Furthermore, mutant pachytene spermatocytes showed normal accumulation of the reciprocal recombination markers, the MutL homologs MLH1 and MLH3, at the sites of crossover (Marcon and Moens, 2003) (Fig. 5B), suggesting that recombination proceeded normally. The overall picture is one of largely normal chromosomal pairing, synapsis, recombination and desynapsis during prophase 1 in the *Ovol1*$^{-/-}$ male mice, indicating that the primary target process of *Ovol1* ablation is cellular differentiation during pachytene.

Molecular consequences of *Ovol1* ablation - a transcriptional profiling comparison of juvenile wild-type and mutant testis

Transcriptional control is key to cellular differentiation. To unravel the gene expression changes caused by *Ovol1* ablation, we performed DNA microarray analysis to compare transcription profiles of wild-type and *Ovol1*$^{-/-}$ testis. Analysis was performed on P16 testis, where apoptosis is minimal. Out of ~11,000 genes analyzed, ~35% were scored as present at this developmental stage in both wild-type and mutant testis. Among these, ~200 RNAs were differentially expressed (upregulated or downregulated) by 1.5-fold or more (P<0.1) between the mutant and wild-type (see Tables S1, S2 in the supplementary material) (a 1.5-fold cut-off was arbitrarily chosen, taking into consideration that microarray experiments tend to underestimate the extent of differential expression). Consistent with the increased number of proliferating germ cells in *Ovol1*$^{-/-}$ testis, several known positive regulators of cellular proliferation were upregulated (see Table S1 in the supplementary material). These include transcription factors Id2 (inhibitor of differentiation 2) and c-Myc/B-myc, signaling molecules such as the mast cell growth factor (Mgf, also known as steel factor or c-kit ligand) and activin (along with its receptor ActR IIB).

Genes that were downregulated in *Ovol1*$^{-/-}$ testis included those whose products are known to be present in pachytene spermatocytes, such as Ldhc4 (see above), Adam2 (also called fertilin β) (Wolfsberg et al., 1995), Tctex2 (Rappold et al., 1987), S-II-T1 (Ito et al., 1996), Odf2 (Turner et al., 1997), Tpx1 (Maeda et al., 1999), Ldha4 (Thomas et al., 1990), Zfp35 (Cunliffe et al., 1990) and acrosin (Kremling et al., 1991) (see Table S2 in the supplementary material). Northern blot analysis of selected markers confirmed their reduced levels in *Ovol1*$^{-/-}$ mutant testis (Fig. 6A). By contrast, the G2-M cell cycle control genes encoding the MPF components Cdc2 and cyclin B1 showed apparently normal levels of mRNA expression in *Ovol1*$^{-/-}$ testis, as detected by transcriptional profiling and northern blot analysis (Fig. 6B). We reasoned that the downregulated genes should include novel pachytene markers, and chose *Ovol2* for additional experiments to test this possibility. Northern blot analysis confirmed that *Ovol2* expression was indeed reduced in juvenile *Ovol1*$^{-/-}$ testis (Fig. 6C), and during normal prepubertal testis development it showed a temporal expression pattern similar to that of *Ovol1* (Li et al., 2002a) (Fig. 6D). Results of in situ hybridization analysis indicated that *Ovol2* expression was activated during mid/late pachytene in wild-type testis (Fig. 6E,F), and that the number of *Ovol2*-expressing (also Ldhc4^{+}) tubules was reduced in *Ovol1*$^{-/-}$ testis (Fig. 6G,H). In tubules that still expressed *Ovol2*, the signal intensity appeared comparable with that in the wild-type (Fig. 6G, compare with 6E). Taken together, these results showing the downregulation of known and novel pachytene differentiation markers in juvenile *Ovol1*$^{-/-}$ testis provide molecular evidence supporting our morphological and biochemical observations of a developmental arrest at the pachytene stage in *Ovol1*$^{-/-}$ male mice.

The microarray analysis also revealed a downregulation of genes such as prominin and Mog1 (see Discussion), the expression of which in testis had not been previously reported. Northern blot analysis confirmed that these genes were indeed expressed in P16 testis, and that their expression was reduced in the *Ovol1*$^{-/-}$ mutant (Fig. 6C). Moreover, both genes showed a temporal expression pattern during normal prepubertal testis development similar to that of *Ovol1* and *Ovol2* (Fig. 6D). This result suggests that their expression is, like that of the *Ovol* genes, normally upregulated during germ cell differentiation. Therefore, our global transcriptional profile analysis also reveals novel, developmentally regulated expression of known genes in testis.

Both in vivo and in vitro evidence indicates that Id2 expression is repressed by Ovol1

To explore the molecular mechanism by which *Ovol1* regulates pachytene differentiation, we sought to identify its downstream target(s). We chose Id2 to focus on, because Id2 protein expression was previously detected in pachytene spermatocytes (Sablitzky et al., 1998) and due to its demonstrated role in spermatogenesis (Yokota, 2001). Northern blot analysis confirmed that the level of Id2 transcripts was higher in juvenile *Ovol1* mutant testis (Fig. 7A). Id2 is also expressed in Sertoli cells (Sablitzky et al., 1998). To rule out the possibility that the increased Id2 transcript level was due to an increased contribution from Sertoli cells, we performed in situ hybridization experiments, which indeed revealed much stronger hybridization signals in *Ovol1*-deficient pachytene spermatocytes than that in the wild type (Fig. 7B, compare signals indicated by arrows in C′ and D′). Furthermore, during normal prepubertal testis development, the temporal expression pattern of Id2 is just the opposite of that of *Ovol1* (Fig. 7C). Taken together, these observations are consistent with the possibility that *Ovol1* represses Id2 expression in normal pachytene spermatocytes.

To further address the above issue, we cloned a mouse Id2 genomic fragment (−1008 to +140, with +1 being the transcription start site) upstream of a luciferase reporter and performed reporter assays in 293T cells. Co-transfection of an *Ovol1* expression vector repressed luciferase expression in a dose-dependent manner (Fig. 7D). We next fused the Ovol1 protein to a strong, well-characterized transactivation domain from VP16 to generate a chimeric protein, VP16-Ovol1. VP16-Ovol1 activated Id2 promoter-luciferase reporter expression in a dose-dependent manner, while the VP16 activation domain alone had no effect (Fig. 7E; data not shown). To address whether repression by Ovol1 or activation by VP16-Ovol1 depends on Ovol1 binding to the Id2 promoter, we examined the promoter sequence and identified a putative Ovol1-binding motif CCGTTA (Li et al., 2002b) that lies 84 bp downstream of the +1 site. This site is conserved between mouse and human (Kurabayashi et al., 1995;Mantani et al., 1998), and was indeed bound by recombinant Ovol1 in gel shift assays (data not shown). The closeness of this Ovol1-binding site to +1 is reminiscent of a key feature of the *Drosophila* Ovo binding sites (Lu and Oliver, 2001). Replacing the CCGTTA sequence with ATGCGC to which Ovol1 does not bind (M.N. and X.D., unpublished) led to both a significant reduction in the degree of repression by Ovol1 and of activation by VP16-Ovol1 (Fig. 7F), indicating that the maximum effect of Ovol1 on Id2 promoter activity requires Ovol1 binding to this site. Collectively, our findings suggest that Ovol1 represses Id2 transcription in a cell-autonomous and direct fashion.

Discussion

Our results demonstrate that *Ovol1* is required for male germ cells to progress through the meiotic pachytene stage. The difference between spermatogenesis and a somatic differentiation process is that the former couples cellular differentiation with meiosis. During the pachytene stage, dramatic changes in gene expression and morphology are interwound with the dynamic, premeiotic chromosomal metabolism. Pachytene spermatocytes not only activate the

expression of genes that are characteristic and/or required for germ cell differentiation, but also elevate the expression levels of genes such as cyclin B1 and Cdc2, which are required for meiotic cell cycle progression (Eddy and O'Brien, 1998). At a morphological level, we observed a reduced number of late-pachytene spermatocytes in *Ovol1* mutant testis, but detected no apparent abnormalities in premeiotic chromosomal behavior. At the biochemical level, *Ovol1*-deficient germ cells failed to properly express pachytene differentiation markers such as Ldhc4, but appeared to maintain at least some aspects of their ability to upregulate the expression of cell cycle control genes such as cyclin B1. The Ldhc4-negative but cyclin B1-positive adluminal germ cells in the mutant testis could be either those that did not exit mitosis, or those that entered meiosis I prematurely. Although the current study does not allow us to unambiguously distinguish between these, our observation of increased number of proliferating germ cells in mutant testis is consistent with the former possibility. Taken together, our results suggest that the primary function of *Ovol1* in meiotic pachytene progression is to regulate the balance between proliferation and differentiation of male germ cells, and exclude a direct involvement of *Ovol1* in premeiotic chromosomal metabolism. This function is somewhat reminiscent of that of several genes in *Drosophila*, the mutation of which caused meiotic pachytene arrest (*can*, *mia* and *sa*), and which are required for the transcription of spermatid differentiation genes but have no effect on cyclin B expression (White-Cooper et al., 1998).

Our work now adds *Ovol1* to a growing list of transcriptional regulators including Egr4 and Mybl1 that are required for meiotic prophase progression in male germ cells (Toscani et al., 1997; Tourtellotte et al., 1999). Distinct from *Egr*4-deficient germ cells, which appeared to arrest at zygotene-early pachytene, *Ovol1*-deficient germ cells stalled at a later stage, i.e., during the early- to late-pachytene transition. Increased germ cell apoptosis, albeit to different extents, was observed in all three (*Egr4*, *Mybl1* and *Ovol1*) mouse models. Assuming that the activity required of these proteins is their transcription regulatory activity, these observations suggest that at least two crucial stages of meiotic prophase are subject to the so-called ‘transcriptional checkpoint’ control (Sassone-Corsi, 1997): the zygotene-pachytene transition and the pachytene stage. Interestingly, although the point of arrest in *Egr*4$^{-/-}$ testis coincides with the time when the synapsis checkpoint is active, the point of arrest in *Ovol1*$^{-/-}$ cells coincides temporally with the pachytene recombination checkpoint (Cohen and Pollard, 2001; Edelmann et al., 1996; Yuan et al., 2001; Yuan et al., 2000). Recombination proceeds normally in the *Ovol1*-deficient germ cells, suggesting that their apoptosis is not due to a recombination failure. However, it remains possible that some common components of the death pathway are activated by recombination errors and *Ovol1* deficiency. It is also interesting to note that ectopic expression of a constitutively nuclear cyclin B1 is sufficient to trigger apoptosis (Porter et al., 2003). In this regard, the precocious nuclear localization of cyclin B1 in *Ovol1*-deficient adluminal germ cells provides a possible mechanism by which *Ovol1* ablation leads to apoptosis.

Our microarray experiments have identified a relatively small number of genes (2%) that are differentially expressed between the juvenile wild-type and *Ovol1*$^{-/-}$ testis. The downregulated genes should provide a useful resource for identifying novel male germ cell or pachytene markers (see Table S2 in the supplementary material). This list includes putative regulatory genes such as transcription factors and signaling molecules, as well as enzymes that are presumably involved in germ cell metabolism. Our northern and in situ hybridization experiments significantly extended our previous finding (Li et al., 2002a) to show that *Ovol2* is a new pachytene marker. Furthermore, the study on the expression of prominin and Mog1 during prepubertal testis development indicates that these genes are expressed in testis in a temporally regulated manner. Prominin encodes a protein that is involved in membrane dynamics and cell shape changes (Roper et al., 2000; Weigmann et al., 1997). Mog1 encodes a guanine nucleotide release factor for Ran GTPase that is known to play a role in nucleocytoplasmic transport of macromolecules and spindle assembly (Clarke and Zhang,

2001; Nicolas et al., 2001). Future studies on the expression and function of these genes in testis should reveal additional insights into the regulation of mammalian spermatogenesis.

The developmental pachytene arrest in *Ovol1*$^{-/-}$ testis is incomplete, as some *Ovol1*-deficient germ cells were able to proceed through the normal differentiation pathway to become functional spermatozoa (Dai et al., 1998). That said, our morphological and biochemical findings were highly reproducible from one mutant mouse to another, and from one genetic background (129XB6) to another (CD1) (data not shown), indicating a clear-cut link between *Ovol1* ablation and these developmental defects. It has been shown that Ovol1 and Ovol2 proteins share 77% sequence identity in the zinc-finger domain and are expressed in overlapping tissues (Dai et al., 1998; Li et al., 2002a; Masu et al., 1998). The co-expression of *Ovol2* with *Ovol1* in pachytene spermatocytes raises the possibility that *Ovol2* can partially compensate for the loss of *Ovol1* function. An ultimate understanding of the full spectrum of Ovol function in mammalian spermatogenesis will require the analysis of *Ovol1*/*Ovol2* double mutants.

The microarray experiments also identified genes that were upregulated in the juvenile *Ovol1*$^{-/-}$ testis. Although previous studies have detected expression of Id2, Myc and Fgf receptors in primary spermatocytes (Cancilla and Risbridger, 1998; Sablitzky et al., 1998; Wolfes et al., 1989), Mgf, activin, Dlk1, Mfge8 and Mif are primarily expressed in somatic cells of the testis (Jensen et al., 1999; Kanai et al., 2000; Meinhardt et al., 2000; Tanaka et al., 2002; Vincent et al., 1998). Therefore, the disruption of *Ovol1* not only affected gene expression in germ cells, but also resulted in alterations of the somatic gene expression program. Undoubtedly, many changes are secondary consequences of the morphological defect. However, genes that are normally expressed in pachytene spermatocytes, such as Id2, are possible intracellular targets of *Ovol1*. Our in situ experiments revealing an upregulation of Id2 transcript level in *Ovol1*-deficient pachytene spermatocytes support a cell-autonomous effect of *Ovol1* on Id2 transcription. This notion is further supported by the in vitro finding that Ovol1 repressed Id2 promoter activity in reporter assays in a dose-dependent manner. Moreover, the extent of repression depends on an Ovol1-binding site that is found in the Id2 promoter and is conserved between mouse and human genes, suggesting that this is a direct repression, and is at least in part mediated by Ovol1 binding to that site. These results, together with the observation that the chimeric protein VP16-Ovol1, in which the only DNA-binding motif is the zinc-finger domain of Ovol1, activated Id2 promoter in a protein dose- and Ovol1 binding site-dependent manner, clearly establish a direct molecular link between *Ovol1* and Id2. Apparently, the identified Ovol1 binding site could not account for all the observed repression, leaving open the existence of additional Ovol1 binding site(s) and/or alternative mechanism(s) of transcriptional regulation by Ovol1. This mechanistic issue merits further study that is outside the scope of this work.

Interestingly, Id2 knockout mice are defective in spermatogenesis (Yokota, 2001). Given the well-demonstrated role of Id2 as a positive regulator of proliferation and a negative regulator of differentiation in multiple cell lineages (Sikder et al., 2003), it is tempting to speculate that a negative regulation of Id2 expression might be a common mechanism by which *Ovol1* promotes cellular differentiation in multiple tissues.

Supplementary Material

Refer to Web version on PubMed Central for supplementary material.

Acknowledgments

We thank Yanhe Lue, Rick Murray and Baogang Xue for helpful advice and technical assistance; Leacky Liaw, Moyra Smith, Ulla Bengtsson and Melanie Oaks for help with microscope use; and Suzanne Sandmeyer and Haoping Liu

for discussions. We are grateful to Erwin Goldberg, George Enders and Mary Ann Handel for kindly providing the α-Ldhc4, α-Gcna1, and α-histone H1t antibodies, respectively. A huge thank you goes to Mary Ann Handel, Wen-Hwa Lee, Grant MacGregor and Rob Steele for critical reading of the manuscript and for valuable suggestions. This work was supported by the NIH Research Grant R01 AR47320 and Basil O'Connor Starter Scholar Research Award Grant Number 5-FY00-547 from the March of Dimes Birth Defects Foundation to X.D. M.N. and D.R.M. were predoctoral trainees supported by the UCI institutional NIH Training Grants on Developmental Mechanisms Underlying Congenital Defects and Structure and Function of Macromolecules, respectively.

References

Bellve AR, Cavicchia JC, Millette CF, O'Brien DA, Bhatnagar YM, Dym M. Spermatogenic cells of the prepuberal mouse. Isolation and morphological characterization. J. Cell Biol 1977;74:68–85. [PubMed: 874003]

Blendy JA, Kaestner KH, Weinbauer GF, Nieschlag E, Schutz G. Severe impairment of spermatogenesis in mice lacking the CREM gene. Nature 1996;380:162–165. [PubMed: 8600391]

Cancilla B, Risbridger GP. Differential localization of fibroblast growth factor receptor-1, -2, -3, and -4 in fetal, immature, and adult rat testes. Biol. Reprod 1998;58:1138–1145. [PubMed: 9603246]

Chapman DL, Wolgemuth DJ. Regulation of M-phase promoting factor activity during development of mouse male germ cells. Dev. Biol 1994;165:500–506. [PubMed: 7958416]

Chu S, Herskowitz I. Gametogenesis in yeast is regulated by a transcriptional cascade dependent on Ndt80. Mol. Cell 1998;1:685–696. [PubMed: 9660952]

Clarke PR, Zhang C. Ran GTPase: a master regulator of nuclear structure and function during the eukaryotic cell division cycle? Trends. Cell Biol 2001;11:366–371. [PubMed: 11514190]

Cobb J, Handel MA. Dynamics of meiotic prophase I during spermatogenesis: from pairing to division. Semin. Cell Dev. Biol 1998;9:445–450. [PubMed: 9813191]

Cobb J, Cargile B, Handel MA. Acquisition of competence to condense metaphase I chromosomes during spermatogenesis. Dev. Biol 1999;205:49–64. [PubMed: 9882497]

Cohen PE, Pollard JW. Regulation of meiotic recombination and prophase I progression in mammals. BioEssays 2001;23:996–1009. [PubMed: 11746216]

Cunliffe V, Koopman P, McLaren A, Trowsdale J. A mouse zinc finger gene which is transiently expressed during spermatogenesis. EMBO J 1990;9:197–205. [PubMed: 2104800]

Dai X, Schonbaum C, Degenstein L, Bai W, Mahowald A, Fuchs E. The ovo gene required for cuticle formation and oogenesis in flies is involved in hair formation and spermatogenesis in mice. Genes Dev 1998;12:3452–3463. [PubMed: 9808631]

Deng W, Lin H. miwi, a murine homolog of piwi, encodes a cytoplasmic protein essential for spermatogenesis. Dev. Cell 2002;2:819–830. [PubMed: 12062093]

Dix DJ, Allen JW, Collins BW, Poorman-Allen P, Mori C, Blizard DR, Brown PR, Goulding EH, Strong BD, Eddy EM. HSP70-2 is required for desynapsis of synaptonemal complexes during meiotic prophase in juvenile and adult mouse spermatocytes. Development 1997;124:4595–4603. [PubMed: 9409676]

Eddy EM. Male germ cell gene expression. Recent Prog. Horm. Res 2002;57:103–128. [PubMed: 12017539]

Eddy EM, O'Brien DA. Gene expression during mammalian meiosis. Curr. Top. Dev. Biol 1998;37:141–200. [PubMed: 9352186]

Edelmann W, Cohen PE, Kane M, Lau K, Morrow B, Bennett S, Umar A, Kunkel T, Cattoretti G, Chaganti R, et al. Meiotic pachytene arrest in MLH1-deficient mice. Cell 1996;85:1125–1134. [PubMed: 8674118]

Edelmann W, Cohen PE, Kneitz B, Winand N, Lia M, Heyer J, Kolodner R, Pollard JW, Kucherlapati R. Mammalian MutS homologue 5 is required for chromosome pairing in meiosis. Nat. Genet 1999;21:123–127. [PubMed: 9916805]

Enders GC, May JJ 2nd. Developmentally regulated expression of a mouse germ cell nuclear antigen examined from embryonic day 11 to adult in male and female mice. Dev. Biol 1994;163:331–340. [PubMed: 8200475]

Eustice DC, Feldman PA, Colberg-Poley AM, Buckery RM, Neubauer RH. A sensitive method for the detection of beta-galactosidase in transfected mammalian cells. Biotechniques 1991;11:739–740. 742-743. [PubMed: 1809326]

Godet M, Thomas A, Rudkin BB, Durand P. Developmental changes in cyclin B1 and cyclin-dependent kinase 1 (CDK1) levels in the different populations of spermatogenic cells of the post- natal rat testis. Eur. J. Cell Biol 2000;79:816–823. [PubMed: 11139145]

Hintz M, Goldberg E. Immunohistochemical localization of LDH-x during spermatogenesis in mouse testes. Dev. Biol 1977;57:375–384. [PubMed: 326599]

Inselman A, Eaker S, Handel MA. Temporal expression of cell cycle-related proteins during spermatogenesis: establishing a timeline for onset of the meiotic divisions. Cytogenet. Genome Res 2003;103:277–284. [PubMed: 15051948]

Ito T, Xu Q, Takeuchi H, Kubo T, Natori S. Spermatocyte-specific expression of the gene for mouse testis-specific transcription elongation factor S-II. FEBS Lett 1996;385:21–24. [PubMed: 8641458]

Jensen CH, Erb K, Westergaard LG, Kliem A, Teisner B. Fetal antigen 1, an EGF multidomain protein in the sex hormone-producing cells of the gonads and the microenvironment of germ cells. Mol. Hum. Reprod 1999;5:908–913. [PubMed: 10508217]

Johnson AD, Fitzsimmons D, Hagman J, Chamberlin HM. EGL-38 Pax regulates the ovo-related gene lin-48 during Caenorhabditis elegans organ development. Development 2001;128:2857–2865. [PubMed: 11532910]

Kanai Y, Kanai-Azuma M, Tajima Y, Birk OS, Hayashi Y, Sanai Y. Identification of a stromal cell type characterized by the secretion of a soluble integrin-binding protein, MFG-E8, in mouse early gonadogenesis. Mech. Dev 2000;96:223–227. [PubMed: 10960788]

Kneitz B, Cohen PE, Avdievich E, Zhu L, Kane MF, Hou H Jr, Kolodner RD, Kucherlapati R, Pollard JW, Edelmann W. MutS homolog 4 localization to meiotic chromosomes is required for chromosome pairing during meiosis in male and female mice. Genes Dev 2000;14:1085–1097. [PubMed: 10809667]

Kremling H, Keime S, Wilhelm K, Adham IM, Hameister H, Engel W. Mouse proacrosin gene: nucleotide sequence, diploid expression, and chromosomal localization. Genomics 1991;11:828–834. [PubMed: 1783391]

Kurabayashi M, Jeyaseelan R, Kedes L. Sequences of the 5′-flanking region of the human helix-loop-helix protein-encoding Id2A gene, and promoter activity regulated by serum and c-Jun/AP-1. Gene 1995;156:311–312. [PubMed: 7758976]

Li B, Dai Q, Li L, Nair M, Mackay D, Dai X. Ovol2, a mammalian homolog of drosophila ovo: gene structure, chromosomal mapping, and aberrant expression in blind-sterile mice. Genomics 2002a; 80:319. [PubMed: 12213202]

Li B, Mackay DR, Dai Q, Li TWH, Nair M, Fallahi M, Schonbaum C, Fantes J, Mahowald A, Waterman ML, et al. The LEF1/β-catenin complex activates *movo*1, a mouse homolog of *Drosophila ovo* gene required for epidermal appendage differentiation. Proc. Natl. Acad. Sci. USA 2002b;99:6064–6069. [PubMed: 11983900]

Lin TY, Viswanathan S, Wood C, Wilson PG, Wolf N, Fuller MT. Coordinate developmental control of the meiotic cell cycle and spermatid differentiation in Drosophila males. Development 1996;122:1331–1341. [PubMed: 8620860]

Liu D, Liao C, Wolgemuth DJ. A role for cyclin A1 in the activation of MPF and G2-M transition during meiosis of male germ cells in mice. Dev. Biol 2000;224:388–400. [PubMed: 10926775]

Long AD, Mangalam HJ, Chan BY, Tolleri L, Hatfield GW, Baldi P. Improved statistical inference from DNA microarray data using analysis of variance and a Bayesian statistical framework. Analysis of global gene expression in Escherichia coli K12. J. Biol. Chem 2001;276:19937–19944. [PubMed: 11259426]

Lu J, Oliver B. Drosophila OVO regulates ovarian tumor transcription by binding unusually near the transcription start site. Development 2001;128:1671–1686. [PubMed: 11290304]

Maeda T, Nishida J, Nakanishi Y. Expression pattern, subcellular localization and structure-function relationship of rat Tpx-1, a spermatogenic cell adhesion molecule responsible for association with Sertoli cells. Dev. Growth Differ 1999;41:715–722. [PubMed: 10646801]

Mantani A, Hernandez MC, Kuo WL, Israel MA. The mouse Id2 and Id4 genes: structural organization and chromosomal localization. Gene 1998;222:229–235. [PubMed: 9831657]

Marcon E, Moens P. MLH1p and MLH3p localize to precociously induced chiasmata of okadaic-acid-treated mouse spermatocytes. Genetics 2003;165:2283–2287. [PubMed: 14704203]

Martianov I, Fimia GM, Dierich A, Parvinen M, Sassone-Corsi P, Davidson I. Late arrest of spermiogenesis and germ cell apoptosis in mice lacking the TBP-like TLF/TRF2 gene. Mol. Cell 2001;7:509–515. [PubMed: 11463376]

Masu Y, Ikeda S, Okuda-Ashitaka E, Sato E, Ito S. Expression of murine novel zinc finger proteins highly homologous to Drosophila ovo gene product in testis. FEBS Lett 1998;421:224–228. [PubMed: 9468311]

Meinhardt A, Bacher M, Wennemuth G, Eickhoff R, Hedger M. Macrophage migration inhibitory factor (MIF) as a paracrine mediator in the interaction of testicular somatic cells. Andrologia 2000;32:46–48. [PubMed: 10702866]

Nantel F, Monaco L, Foulkes NS, Masquilier D, LeMeur M, Henriksen K, Dierich A, Parvinen M, Sassone-Corsi P. Spermiogenesis deficiency and germ-cell apoptosis in CREM-mutant mice. Nature 1996;380:159–162. [PubMed: 8600390]

Nicolas FJ, Moore WJ, Zhang C, Clarke PR. XMog1, a nuclear ran-binding protein in Xenopus, is a functional homologue of Schizosaccharomyces pombe mog1p that co-operates with RanBP1 to control generation of Ran-GTP. J. Cell Sci 2001;114:3013–3023. [PubMed: 11686304]

Oliver B, Pauli D, Mahowald AP. Genetic evidence that the ovo locus is involved in Drosophila germ line sex determination. Genetics 1990;125:535–550. [PubMed: 2116356]

Payre F, Vincent A, Carreno S. ovo/svb integrates Wingless and DER pathways to control epidermis differentiation. Nature 1999;400:271–275. [PubMed: 10421370]

Pear WS, Nolan GP, Scott ML, Baltimore D. Production of high-titer helper-free retroviruses by transient transfection. Proc. Natl. Acad. Sci. USA 1993;90:8392–8396. [PubMed: 7690960]

Pearse RV 2nd, Drolet DW, Kalla KA, Hooshmand F, Bermingham JR Jr, Rosenfeld MG. Reduced fertility in mice deficient for the POU protein sperm-1. Proc. Natl. Acad. Sci. USA 1997;94:7555–7560. [PubMed: 9207130]

Pines J, Hunter T. Human cyclins A and B1 are differentially located in the cell and undergo cell cycle-dependent nuclear transport. J. Cell Biol 1991;115:1–17. [PubMed: 1717476]

Porter LA, Cukier IH, Lee JM. Nuclear localization of cyclin B1 regulates DNA damage-induced apoptosis. Blood 2003;101:1928–1933. [PubMed: 12424202]

Rappold GA, Stubbs L, Labeit S, Crkvenjakov RB, Lehrach H. Identification of a testis-specific gene from the mouse t-complex next to a CpG-rich island. EMBO J 1987;6:1975–1980. [PubMed: 3653077]

Roper K, Corbeil D, Huttner WB. Retention of prominin in microvilli reveals distinct cholesterol-based lipid micro-domains in the apical plasma membrane. Nat. Cell Biol 2000;2:582–592. [PubMed: 10980698]

Sablitzky F, Moore A, Bromley M, Deed RW, Newton JS, Norton JD. Stage- and subcellular-specific expression of Id proteins in male germ and Sertoli cells implicates distinctive regulatory roles for Id proteins during meiosis, spermatogenesis, and Sertoli cell function. Cell Growth Differ 1998;9:1015–1024. [PubMed: 9869302]

Sassone-Corsi P. Transcriptional checkpoints determining the fate of male germ cells. Cell 1997;88:163–166. [PubMed: 9008156]

Shuster EO, Byers B. Pachytene arrest and other meiotic effects of the start mutations in Saccharomyces cerevisiae. Genetics 1989;123:29–43. [PubMed: 2680756]

Sikder HA, Devlin MK, Dunlap S, Ryu B, Alani RM. Id proteins in cell growth and tumorigenesis. Cancer Cell 2003;3:525–530. [PubMed: 12842081]

Sucena E, Delon I, Jones I, Payre F, Stern DL. Regulatory evolution of shavenbaby/ovo underlies multiple cases of morphological parallelism. Nature 2003;424:935–938. [PubMed: 12931187]

Tanaka Y, Taniyama H, Tsunoda N, Shinbo H, Nagamine N, Nambo Y, Nagata S, Watanabe G, Herath CB, Groome NP, et al. The testis as a major source of circulating inhibins in the male equine fetus during the second half of gestation. J. Androl 2002;23:229–236. [PubMed: 11868816]

Thepot D, Weitzman JB, Barra J, Segretain D, Stinnakre MG, Babinet C, Yaniv M. Targeted disruption of the murine junD gene results in multiple defects in male reproductive function. Development 2000;127:143–153. [PubMed: 10654608]

Thomas K, Del Mazo J, Eversole P, Bellve A, Hiraoka Y, Li SS, Simon M. Developmental regulation of expression of the lactate dehydrogenase (LDH) multigene family during mouse spermatogenesis. Development 1990;109:483–493. [PubMed: 2401207]

Toscani A, Mettus RV, Coupland R, Simpkins H, Litvin J, Orth J, Hatton KS, Reddy EP. Arrest of spermatogenesis and defective breast development in mice lacking A-myb. Nature 1997;386:713–717. [PubMed: 9109487]

Tourtellotte WG, Nagarajan R, Auyeung A, Mueller C, Milbrandt J. Infertility associated with incomplete spermatogenic arrest and oligozoospermia in Egr4-deficient mice. Development 1999;126:5061–5071. [PubMed: 10529423]

Tung KS, Hong EJ, Roeder GS. The pachytene checkpoint prevents accumulation and phosphorylation of the meiosis-specific transcription factor Ndt80. Proc. Natl. Acad. Sci. USA 2000;97:12187–12192. [PubMed: 11035815]

Turner KJ, Sharpe RM, Gaughan J, Millar MR, Foster PM, Saunders PT. Expression cloning of a rat testicular transcript abundant in germ cells, which contains two leucine zipper motifs. Biol. Reprod 1997;57:1223–1232. [PubMed: 9369191]

Vincent S, Segretain D, Nishikawa S, Nishikawa SI, Sage J, Cuzin F, Rassoulzadegan M. Stage-specific expression of the Kit receptor and its ligand (KL) during male gametogenesis in the mouse: a Kit-KL interaction critical for meiosis. Development 1998;125:4585–4593. [PubMed: 9778516]

Wang X, Chamberlin HM. Multiple regulatory changes contribute to the evolution of the Caenorhabditis lin-48 ovo gene. Genes Dev 2002;16:2345–2349. [PubMed: 12231624]

Weigmann A, Corbeil D, Hellwig A, Huttner WB. Prominin, a novel microvilli-specific polytopic membrane protein of the apical surface of epithelial cells, is targeted to plasmalemmal protrusions of non-epithelial cells. Proc. Natl. Acad. Sci. USA 1997;94:12425–12430. [PubMed: 9356465]

White-Cooper H, Schafer MA, Alphey LS, Fuller MT. Transcriptional and post-transcriptional control mechanisms coordinate the onset of spermatid differentiation with meiosis I in Drosophila. Development 1998;125:125–134. [PubMed: 9389670]

Wolfes H, Kogawa K, Millette CF, Cooper GM. Specific expression of nuclear proto-oncogenes before entry into meiotic prophase of spermatogenesis. Science 1989;245:740–743. [PubMed: 2475907]

Wolfsberg TG, Straight PD, Gerena RL, Huovila AP, Primakoff P, Myles DG, White JM. ADAM, a widely distributed and developmentally regulated gene family encoding membrane proteins with a disintegrin and metalloprotease domain. Dev. Biol 1995;169:378–383. [PubMed: 7750654]

Yokota Y. Id and development. Oncogene 2001;20:8290–8298. [PubMed: 11840321]

Yuan L, Liu JG, Zhao J, Brundell E, Daneholt B, Hoog C. The murine SCP3 gene is required for synaptonemal complex assembly, chromosome synapsis, and male fertility. Mol. Cell 2000;5:73–83. [PubMed: 10678170]

Yuan L, Liu JG, Hoja MR, Lightfoot DA, Hoog C. The checkpoint monitoring chromosomal pairing in male meiotic cells is p53-independent. Cell Death Differ 2001;8:316–317. [PubMed: 11319615]

Zhang D, Penttila TL, Morris PL, Teichmann M, Roeder RG. Spermiogenesis deficiency in mice lacking the Trf2 gene. Science 2001;292:1153–1155. [PubMed: 11352070]

Zhao R, Gish K, Murphy M, Yin Y, Notterman D, Hoffman WH, Tom E, Mack DH, Levine AJ. Analysis of p53-regulated gene expression patterns using oligonucleotide arrays. Genes Dev 2000;14:981–993. [PubMed: 10783169]

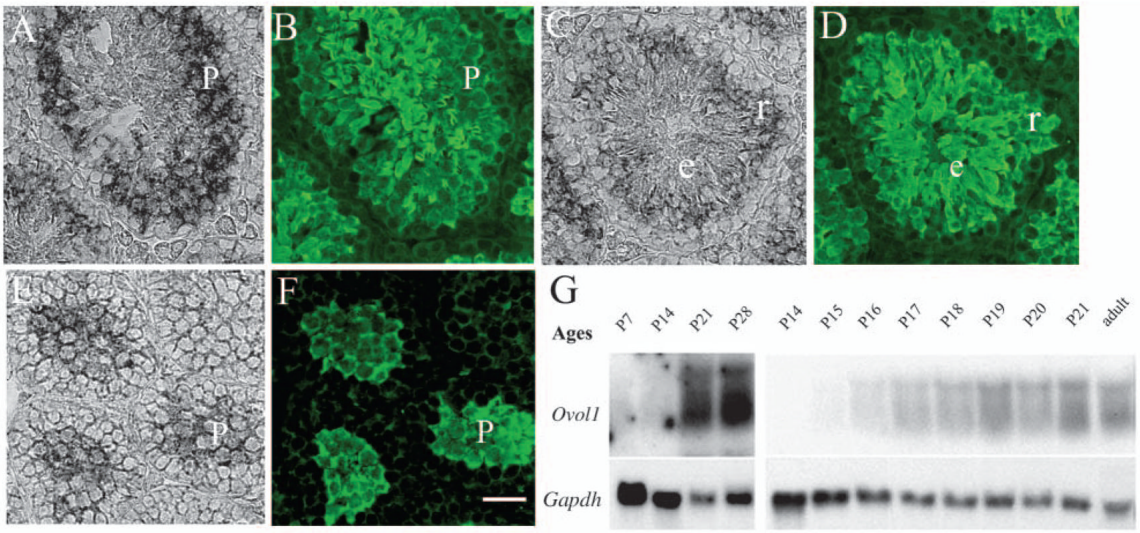

Fig. 1.

Ovol1 RNA expression in adult and prepubertal testis. (A-F) In situ hybridization of testis from 8-week-old (A-D) or 16-day-old (E,F) mice using a *Ovol1* cRNA probe (A,C,E), or counterstained with an a-Ldhc4 antibody (B,D,F). The following stages were identified according to cell sizes, positions within the tubule and relative intensities of α-Ldhc4 staining (Hintz and Goldberg, 1977): p, pachytene spermatocytes; r, round spermatids; e, elongate spermatids. No hybridization signal was observed using a sense probe (not shown). (G) Northern blot analysis detecting multiple *Ovol1* transcripts in testis during prepubertal development. Numbers at the top of each lane indicate the postnatal ages at which testis samples were taken. The same blots were then stripped and hybridized with a Gapdh probe. Scale bar: 25 μm in A-D; 30 μm in E-F.

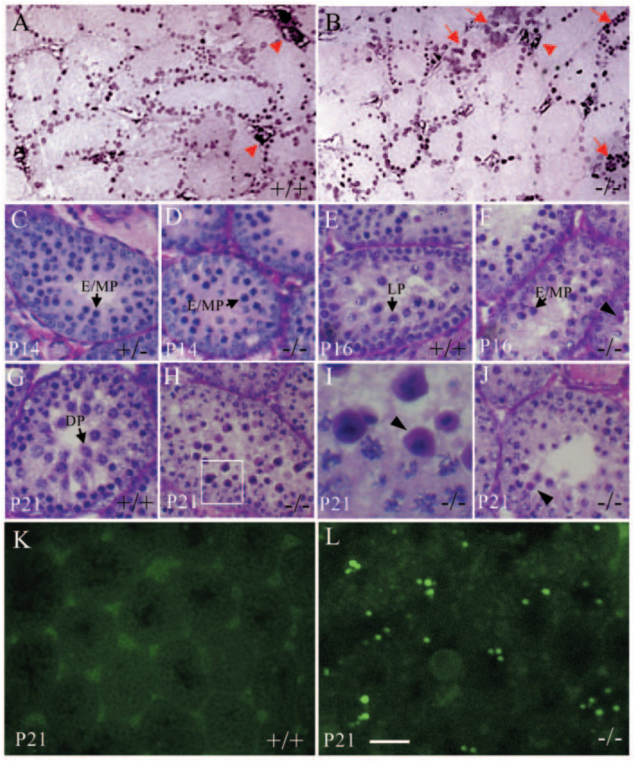

Fig. 2.

Proliferation, morphology and apoptosis in juvenile *Ovol1*$^{-/-}$ testis. (A,B) BrdU labeling of testis from P14 wild-type (A) and *Ovol1*$^{-/-}$ (B) mice. Arrows indicate seminiferous tubules that contain multiple rows of BrdU-positive germ cells. Arrowheads indicate the labeled Leydig cells. (C-J) PAS staining of testis from control (wild-type or *Ovol1*$^{+/-}$) (C,E,G) and *Ovol1*$^{-/-}$ (D,F,H-J) mice at P14, P16 and P21. E/MP, early/mid-pachytene spermatocytes; DP, diplotene spermatocytes. (I) High-magnification image of the boxed area in H. Black arrowheads in F,I,J indicate apoptotic cells intermingled with late-pachytene spermatocytes or more advanced germ cells. (K,L) TUNEL assays on wild-type (K) and mutant (L) testis from 21-day-old mice. Scale bar: 80 μm in A,B; 35 μm in C-H,J; 9 μm in I; 100 μm in K,L.

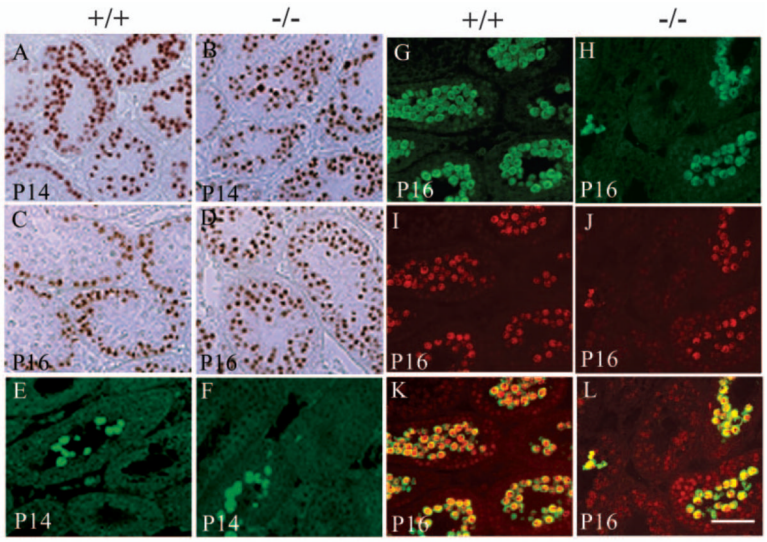

Fig. 3.

Accumulation of Gcna1^{+} germ cells and reduction of Ldhc4^{+}/histone H1t^{+} germ cells in testis of juvenile *Ovol1*$^{-/-}$ mice.

(A-D) Immunohistochemical detection of the Gcna1 protein in testis from *Ovol1*$^{+/+}$ (A,C) and *Ovol1*$^{-/-}$ (B,D) mice at P14 and P16 using an α-Gcna1 antibody.

(E-L) Immunofluorescence staining of testis from *Ovol1*$^{+/+}$ (E,G,I,K) and *Ovol1*$^{-/-}$ (F,H,J,L) mice at P14 and P16 using an α-Ldhc4 antibody (E-H) and an α-histone H1t antibody (I,J).

(K,L) Merged images between G and I, and H and J, respectively. Scale bar: 55 μm in A-F; 60 μm in G-L.

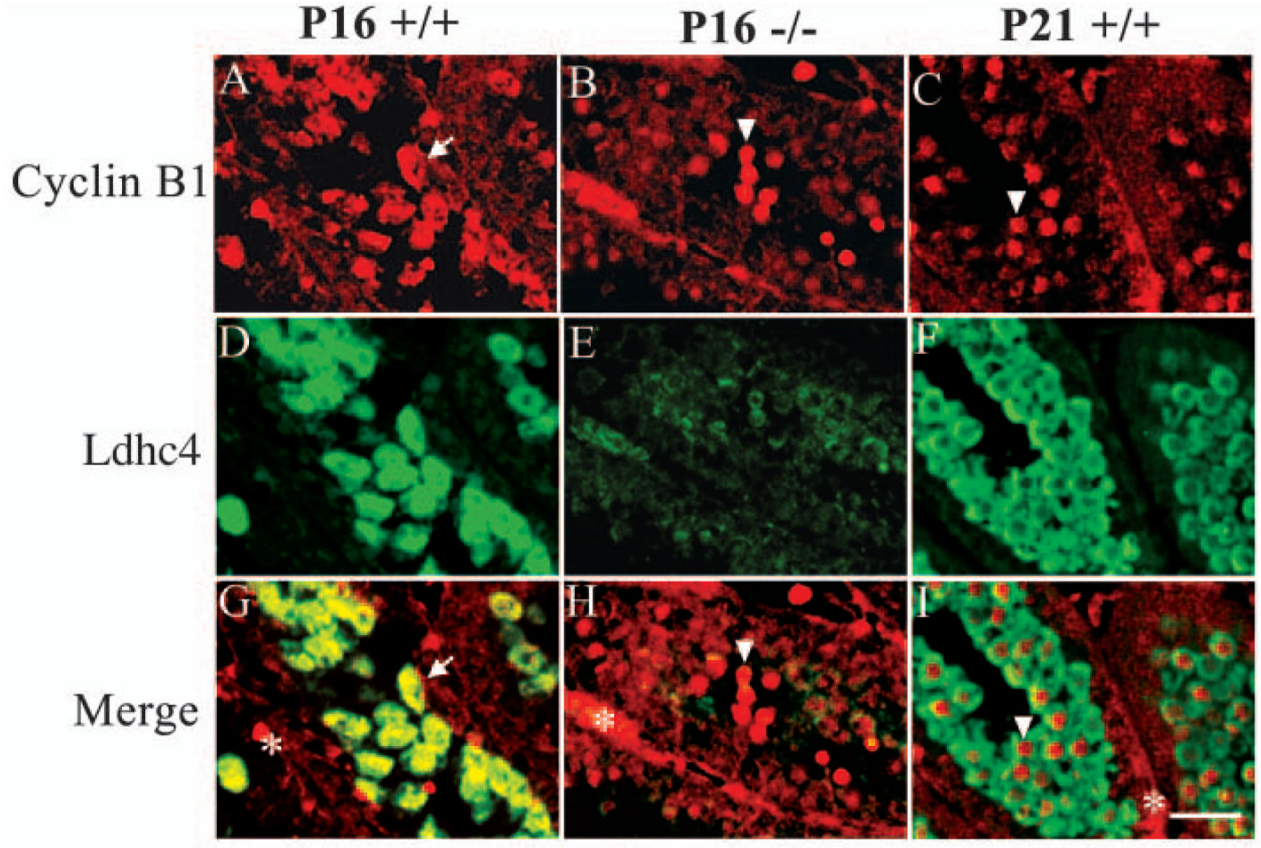

Fig. 4.

Expression and localization of cyclin B1 protein in wild-type (A,C,D,F,G,I) and *Ovol1*$^{-/-}$ (B,E,H) testis. Shown are results of immunostaining experiments using αcyclin B1 (A-C) and αLdhc4 (D-F) antibodies on P16 (A,B,D,E,G,H) and P21 (C,F,I) testis. (G-I) Merged images. Asterisk in G-I indicates mitotic spermatogonia at the tubule periphery that stained positive for cyclin B1. Arrows and arrowheads indicate cytoplasmic and nuclear cyclin B1 in primary spermatocytes, respectively. Scale bar: 25 μm.

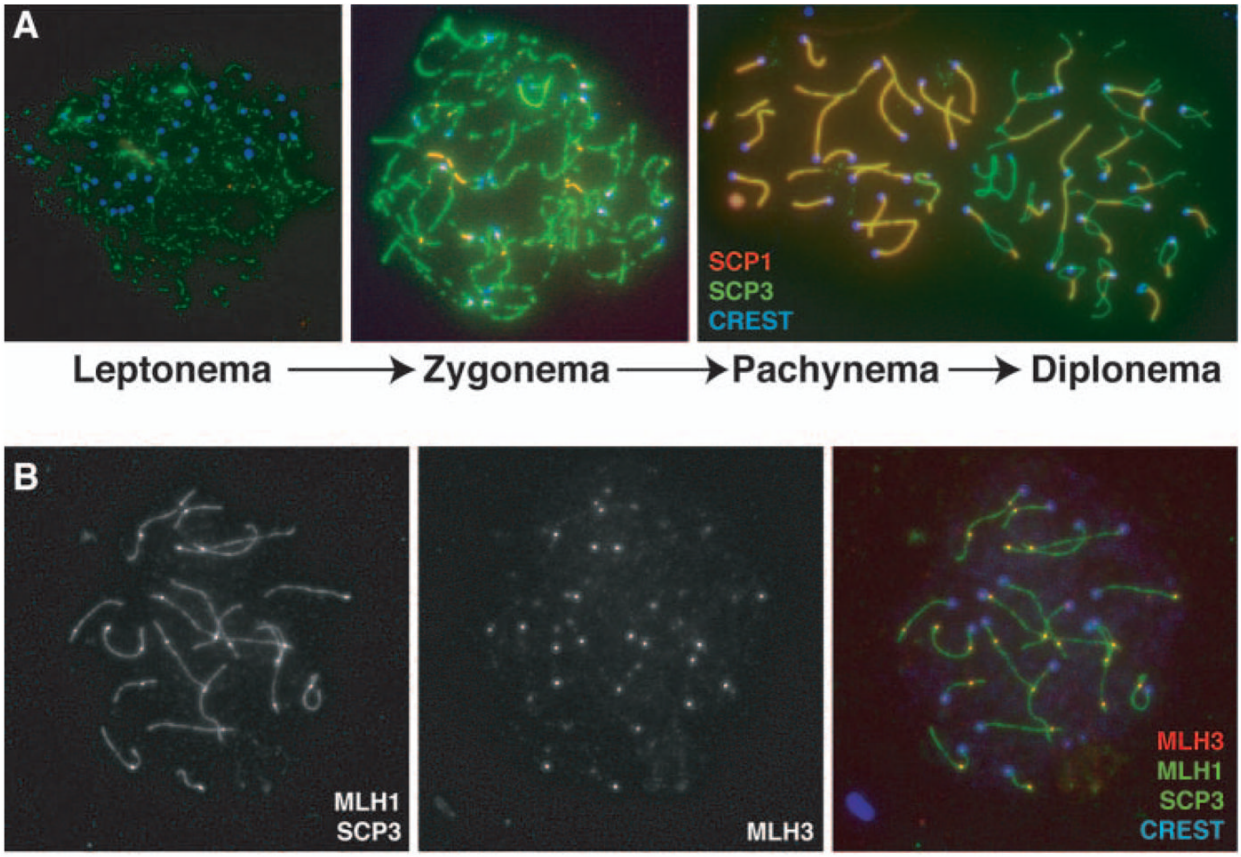

Fig. 5.

Spermatocyte spread preparations from *Ovol1*$^{-/-}$ males showing normal cytological progression through prophase I (A) and normal accumulation of MLH1 and MLH3 at pachynema of prophase I (B). In the top panels (A), the accumulation of SCP3 (in green) along chromosomes begins in leptonema and continues through zygonema, at which time SCP1 (in red) begins to accumulate and results in homologous chromosome synapsis (double staining resulted in 'yellow' chromosomes). By pachynema, all autosomes are fully synapsed, and the XY bivalent is synapsed only at the pseudoautosomal region. At diplonema, the central element of the synaptonemal complex breaks down and the SCP3-associated homologs move apart, but remain attached at sites of chiasmata (these sites are still associated with SCP1 at this time). In the bottom panels (B), the progression of recombination is associated with the accumulation of MLH1 (green in the last panel) and MLH3 (red) on the SCP3-positive (fainter green) chromosome cores in a manner identical to that in the wild-type control littermates (not shown). Colocalization of MLH1 and MLH3 is evident (as indicated by bright yellow spots along the chromosomes). In all panels, the telocentric centromere is indicated by CREST immunostaining (blue).

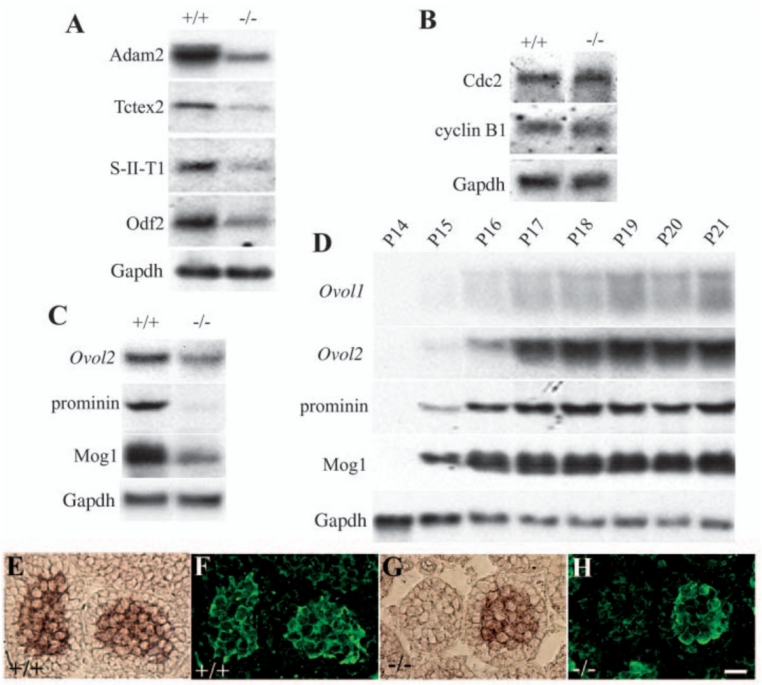

Fig. 6.

Altered gene expression in *Ovol1*$^{-/-}$ testis. (A) Reduced expression of known pachytene differentiation markers in P16 *Ovol1*$^{-/-}$ testis. (B) Northern blot analysis showing apparently normal levels of cyclin B1 and Cdc2 transcripts in P16 *Ovol1*$^{-/-}$ testis. (C,D) Novel pachytene or testis markers were downregulated in P16 *Ovol1*$^{-/-}$ testis (C) and showed temporal expression patterns similar to that of *Ovol1* during wild-type prepubertal testis development (D). RNA samples were pooled from three to five mice of the same genotype and used to make multiple blots. All blots were stripped and reused. Only one representative hybridization experiment with a Gapdh probe was shown as a loading control. (E-H) In situ hybridization of P16 wild-type (E,F) and *Ovol1*$^{-/-}$ (G,H) testis using a *Ovol2* cRNA probe (E,G) or counterstained with an a-Ldhc4 antibody (F,H). *Ovol2* transcripts are present in Ldhc4-postive cells. No signal was detected when a sense probe was used (not shown). Scale bar: 30 μm.

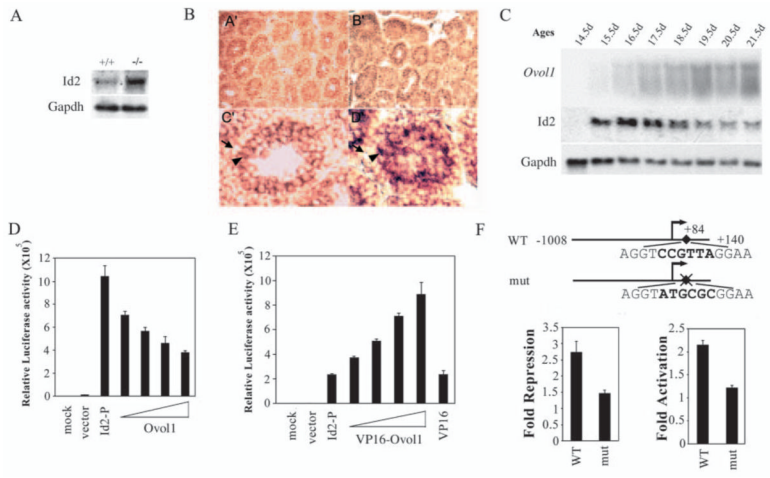

Fig. 7.

Id2 transcription is upregulated in *Ovol1*-deficient germ cells and is repressed by Ovol1 protein in vitro. (A) Increased levels of Id2 mRNA in P16 *Ovol1*$^{-/-}$ testis. (B) In situ hybridization of P16 wild-type (A′,C′) and *Ovol1*$^{-/-}$ (B′,D′) testis using an Id2 cRNA probe. (C′ and D′) High magnification images of individual tubules showing the strongest Id2 expression. Arrowheads and arrows indicate the Id2-expressing primary spermatocytes and the non-expressing spermatogonia, respectively. (C) Temporal expression of Id2 during normal prepubertal testis development. (D) Repression of Id2 promoter (Id2-P)-luciferase reporter expression by Ovol1. (E) Activation of Id2-P-luciferase expression by VP16-Ovol1. The triangles indicate increasing concentrations of expression vectors. The VP16 alone control is at a concentration corresponding to the highest one used for VP16-Ovol1. (F) Repression or activation is partially dependent on the CCGTTA sequence in Id2 promoter. Each bar represents the average of triplicate samples in a single experiment, and results are representative of several independent experiments. Luciferase activities are normalized for transfection efficiency by using a β-actin promoter driving *lacZ* as an internal control.

Table 1

Frequency distribution of pachytene, Gcna1$^+$ and Ldhc4$^+$ spermatocytes in juvenile *Ovol1*$^{-/-}$ and wild-type control testis

Age	**P14**		**P16**	
Genotype	**+/+**	**−/−**	**+/+**	**−/−**
Average tubule diameter* (μm)	79.8±6.0	76.0±4.7	91.1±5.1	83.3±7.5
Pachytene /total germ cells (%‡)	210/1570 (13.4%)	222/1559 (14.2%)	452/1564 (28.9%)	470/1694 (27.7%)
Late pachytene§	0	0	106±7	49±8
Gcna1$^+$ cells¶	1185±24	1188±15	852±16	1258±55
Ldhc4$^+$ cells¶	88±4	81±7	493±23	185±14

*Determined by measuring a total of 40 neighboring tubules.

†Refers to the total number of spermatocytes that are at the pachytene stage (including early-, mid- and late-) from an area of 2×10^5 μm^2 in size (equivalent to ~25 tubular cross-sections).

‡Refers to the percentage of pachytene spermatocytes in the total number of germ cells in that area.

§The total number of late-pachytene spermatocytes (scored by the large size of their nuclei or the presence of the ‘sex body’) in an area of 2×10^5 μm^2 was calculated as an average of four independent areas.

¶Measured from the same-size areas as above.